Selective Adsorption of Serum Albumin on Biomedical Polyurethanes Modified by a Poly(ethylene oxide) Coupling-Polymer with Cibacron Blue (F3G-A) Endgroups

Dong-an Wang,*[,†,‡] Bao-lin Chen,[†,§] Jian Ji,[†] and Lin-xian Feng[†,||]

Department of Polymer Science and Engineering, Zhejiang University, Hangzhou, 310027, P. R. China, Department of Pharmaceutical Sciences, University of Tennessee Health Science Center, Memphis, Tennessee 38163, and Department of Chemistry, Inner Mongolia Hulunbeier Collage, Hailaer, 021008, P. R. China . Received January 22, 2002; Revised Manuscript Received April 3, 2002

A tri-*block*-coupling polymer, "PEO−MDI−PEO" ["poly(ethylene oxide)−4,4′-methylene diphenyl diisocyanate−poly(ethylene oxide)", abbreviated "MPEO"], was used to react with a triazine dye, Cibacron Blue F3G-A (ciba), in an alkaline environment. The product of this nucleophilic reaction was a penta-*block*-coupling polymer, "ciba-PEO-MDI-PEO-ciba" (abbreviated "cibaMPEO"). The cibaMPEO-modified poly(ether urethane) (PEU) surfaces were prepared by dip-coating and detected by XPS. The surface enrichment of both ciba endgroups and poly(ethylene oxide) spacer-arms was revealed. On the modified surfaces, bovine serum albumin (BSA)-adsorbing experiments were carried out, respectively, in the low and high BSA bulk-concentration solutions, and accordingly, the methods of radioactive ^{125}I-probe and ATR-FTIR were, respectively, employed for the characterization. The competitive adsorption of BSA and bovine serum fibrinogen (Fg) in the BSA−Fg binary solutions was also studied using a ^{125}I-probe, and through which the reversibly BSA-selective adsorption on cibaMPEO-modified PEU surfaces was confirmed. Finally, the improvement of blood-compatibility on the modified surfaces was verified by the plasma recalcification time (PRT) test.

INTRODUCTION

The implantable biomedical devices made of polymeric materials, such as blood-contacting intravascular catheters, have been extensively utilized for the interventional treatments in clinical practice. However, the surfaces of these devices may promote the in situ blood coagulation, microbial infections, and consequent inflammatory reactions (*1*, *2*). It is believed that these iatrogenic effects are likely to be mediated by adsorbed host proteins on the device surfaces (*3*, *4*). It is also widely accepted that albumin-coated surfaces can minimize those harmful effects (*5*, *6*). Thus, a series of novel surface-modifying additives (SMA) were specially designed to develop surfaces that would selectively bind the host albumin.

In our study, a triazine dye, Cibacron Blue F3G-A (abbreviated "ciba") (Schemes 1, 2) and the polymeric material poly(ethylene oxide) (PEO) were employed as the two main components of the SMA. Ciba possesses the capacity to selectively bind the host albumin. It is proposed that the binding of ciba to human serum albumin (HSA) is at the bilirubin-binding sites and ciba's binding to bovine serum albumin (BSA) is at the fatty acid-binding sites (*7*, *8*). PEO is a well-known and very useful biomaterial. Under aqueous physiological conditions, hydrophilic PEO has high kinetic chain mobility and large thermodynamical steric volume (*9*), leading to the repulsion of almost all kinds of foreign adherence and adsorption. Accordingly, for the SMA in our study, ciba was introduced as the functional endgroup, and the PEO chains were employed as the spacer-arms. We hypothesize that on the modified surface, ciba will selectively bind the host albumin, while the PEO will be resistant to the adsorption of the tangible humoral (particularly haemal) components such as proteins and cells. As the endgroup, ciba's presence on the blood−polymer interface would depend on the support from the hydrophilic PEO backbones, and the activity of ciba would also be provided by the mobility of PEO chains. Because of this proposed cooperative effect between the PEO spacer and ciba endgroup of SMA, the biocompatibility of the medical device was expected to be improved.

The SMA in our study is a penta-*block*-coupling polymer of "ciba−PEO−4,4′-methylene diphenyl diisocyanate (MDI)−PEO−ciba" (abbreviated "cibaMPEO") (Schemes 1, 2), which was a product of the nucleophilic reaction between ciba and the preproduct, a tri-*block*-coupling polymer of "PEO−MDI−PEO" (abbreviated "MPEO") (Scheme 1) (*10*, *11*). The matrix material of the medical device in this paper was poly(ether urethane) (PEU). The expedient dip-coating method of surface modification was selected. According to the conclusions from our earlier studies (*10*, *11*), H-bonds will be formed between the middle MDI-blocks of cibaMPEO and the "hard" blocks of PEU chains (Scheme 2), by which the stability of the coating can be ensured.

The adsorbing experiments of BSA and/or fibrinogen (Fg) were carried out on the modified surfaces. The systemic quantitative analysis was performed using attenuated total reflection (ATR) FT-IR spectroscopy (*12*, *13*) for the experiments with high BSA-bulk-concentra-

* Current address of the corresponding author: Dong-an Wang, Ph.D., Department of Pharmaceutical Sciences, University of Tennessee Health Science Center, 26 South Dunlap St., Room 406, Memphis, TN 38163, Tel: (901) 448-6848, Fax: (901) 448-6092, E-mail: danielwda@netzero.net.

† Zhejiang University.

‡ University of Tennessee Health Science Center.

§ Inner Mongolia Hulunbeier Collage.

|| Deceased on July 26, 2001.

10.1021/bc0255079 CCC: $22.00
Published on Web 06/22/2002

Scheme 1. Synthesis Routes of MPEOs and CibaMPEOs

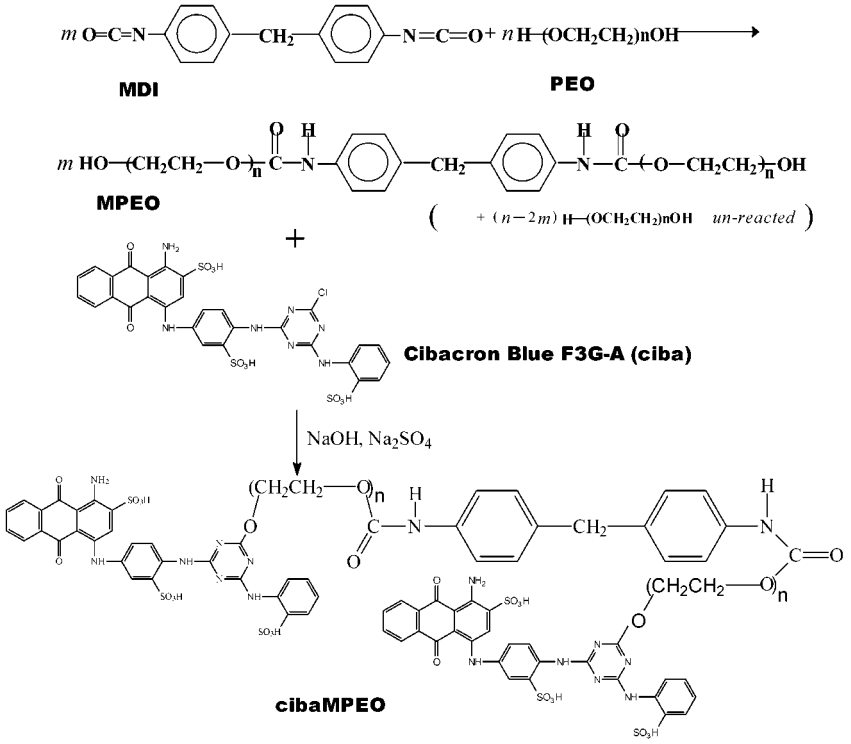

tion solutions and using a radioactive ^{125}I-labeled probe (*8*) for the experiments with low BSA- and/or Fg-bulk-concentration solutions. Finally, for characterization of anticoagulation, measurements of plasma recalcification time (PRT) (*14*) were carried out.

EXPERIMENTAL SECTION

Preparation of SMA−CibaMPEO and Modified PEU Surfaces. *Preparation of MPEO and CibaMPEO.*The synthesis and purification of MPEO (PEO MW 1000, 2000, 6000, and 10000; the corresponding MPEO were named MPEO1k, -2k, -6k, and -10k) were reported previously (*10*). The preparation of SMA−cibaMPEO (Scheme 1) was based on the nucleophilic substitution of the Cl^- on ciba (Cibacron Blue; purchased from Sigma Chemical Co., St. Louis, MO, C9534) by MPEO's hydroxyl endgroup (*15*). MPEO (MPEO1k, -2k, -6k, and 10k, respectively, 5.0 g) and ciba (accordingly 1.00, 0.5, 0.33, and 0.10 g) were dissolved in deionized water (10 mL) with NaOH (1.12 g) and anhydrous Na_2SO_4 (0.48 g). The mixture was moderately stirred at room temperature for 12 h. Ice-cold acetic acid (1.6 mL) was added to terminate the reaction by neutralizing the medium. The product was dried over magnesium sulfate and concentrated in vacuo. The residue was further dried under high vacuum overnight at 60 °C. The resulting blue powders were washed and filtered with tetrahydrofuran to remove the insoluble salts and unreacted ciba. Finally, graded precipitation was carried out with ethyl ether to isolate the desired blue products from the unreacted MPEO, which was monitored by the resulting color and GPC (Baseline 810 method, Waters). The corresponding final products were respectively named cibaMPEO1k, -2k, -6k, and 10k. ^{1}H NMR spectroscopy (500 MHz, AVANCE DMX500, Bruker; solvent DMSO-d_6, Aldrich) and XPS (ADXPS, VG Instruments) were used for characterization.

Preparation of CibaMPEO-Modified PEU Surfaces. The sheets (80 mm × 10 mm × 2 mm) of poly(ether urethane) (PEU, Pellethane 2363−80AE, Dow Chemical) were used as the matrix material, and the PEU pellets were used as the film-building additive (FBA) for coating. FBA−PEU has been extracted with alcohol in a soxhlet extractor for 72 h to remove the processing aid (stearamide additive) (*16*). The coating solution was obtained by dissolving SMA−cibaMPEO and FBA−PEU together into tetrahydrofuran and then diluting with equal volume of alcohol. The dosage ratio of cibaMPEO/PEU was 3:2 (w/w), and the concentration of cibaMPEO was 4% (w/v). The dip-coating process was performed on an electric lifter. The matrix-PEU sheets were vertically dipped into and then lifted out of the coating solution with constant speed followed by drying in a vacuum for 30 min. The process was repeated three times. Two kinds of control sample, which was respectively coated only with the FBA−PEU or only with MPEO/FBA−PEU, were also prepared. XPS was used to analyze the modified PEU surfaces (PEU-control, ctMPEO2k, ct-cibaMPEO1k, -2k, -6k, and -10k).

Preparation of Protein-Adsorbed Surfaces. *Proteins and Buffers.* Bovine serum albumin (BSA) was provided by Sigma (A-2153, protein content 96−99%, M_n 66,210, refraction index $n_2 = 1.5$ at infrared absorbance 1550 cm^{-1} (*12*)). Bovine serum fibrinogen (Fg) was also from Sigma (F-8630, protein content 74% (Biuret), clottable protein 87%, 10% sodium citrate, 15% NaCl). Fg was purified by dialysis with dialysis sacks (Sigma 250-7U, retains proteins with $M_n > 12000$) and stored under −20 °C. The tris(hydroxyethyl)methylaminomethane (A.R., abbreviated "Tris") and glycine (A.R., abbreviated "Gly") were from Shanghai Bio-Chem. Co. The buffers of "Tris-HCl" solution (6.057 g Tris/water 1000 mL, pH 7.35−7.40) and "Gly-NaOH" solution (6 g Gly/water 80 mL, pH 8.80) were prepared. The Gly-NaOH buffer was stored under 4 °C. All the water used was double-distilled deionized water.

Radioactive Protein Probe. Radioactive Na^{125}I (25 mCi, original radiointensity 160−180 mCi/mL, without reductives, $t_{1/2}$ = 59.7 d) was provided by the Institute of

Scheme 2. Schematic Representation of the H Bond Incorporation between CibaMPEO and PEU

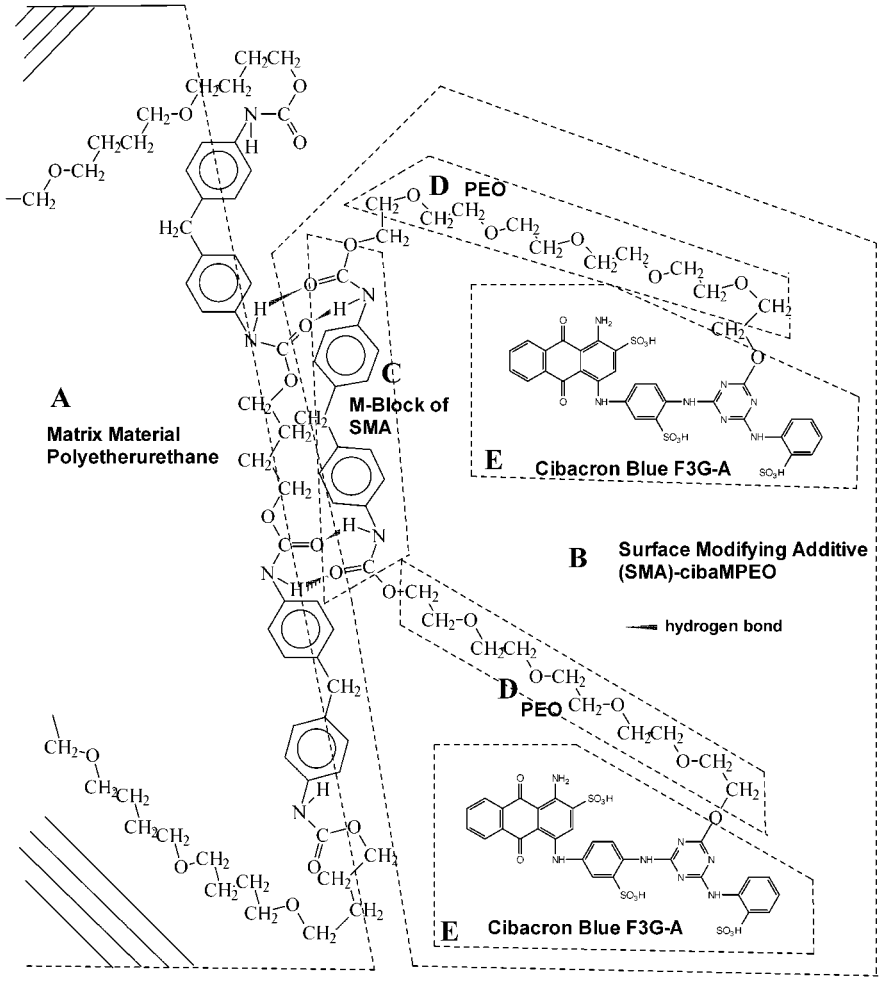

Scheme 3. Methods of Quantitative Characterization of (a) Protein-Adsorbed Samples and (b) Standard Protein Solutions by ATR-FT-IR

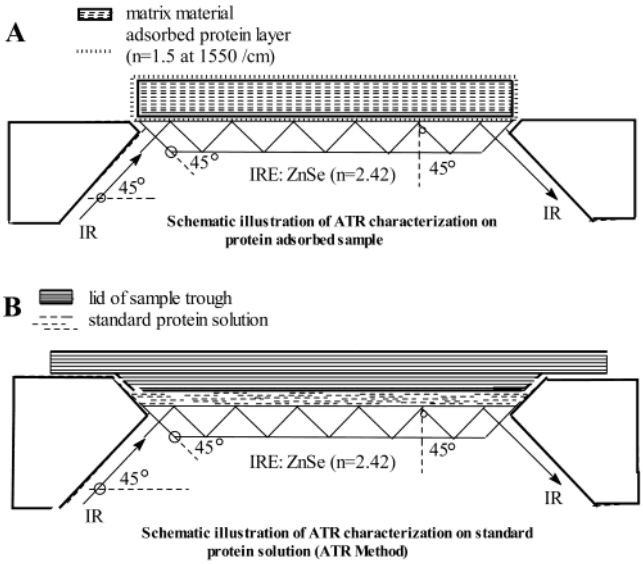

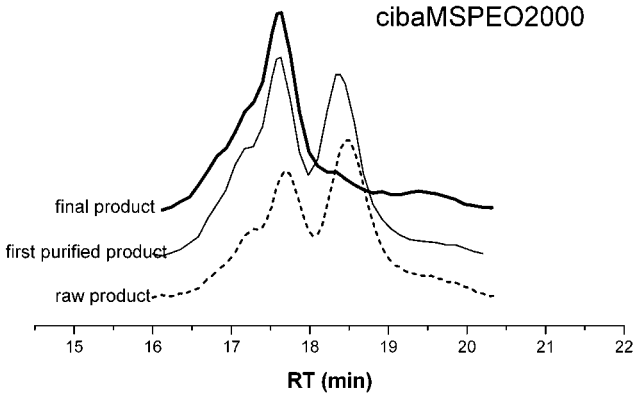

Figure 1. GPC spectra of cibaMPEO(2k) for the purification. The chromatographic peaks at approximately 17.5 min (RT) represent the product cibaMPEO; the peaks at approximately 18.5 min (RT) represent the unreacted MPEO.

Atomic Energy of China and was used within the first half of $t_{1/2}$. The preparation of ICl solution and the following ^{125}I-labeling of the protein were reported elsewhere (*17*). The radioactive protein probe was acquired by mixing the solution of protein (4 mg/0.1 mL) in Gly-NaOH into the solution of 0.01 mL of ICL/0.5 of mL Gly-NaOH/Na^{125}I (Na^{125}I dosage for BSA 0.2 mCi, for Fg 0.1 mCi) and then eluting with Tris-HCl through an alkali PS anion exchanger column (Shanghai Chemical Co.).

Protein Solutions. As for the protein-bulk-solution for adsorption and/or the protein-standard-solution for the calculation, the BSA, Fg, and the BSA−Fg binary solutions were respectively prepared in Tris-HCl buffer. The radioactive bulk solution was prepared by adding the radioactive protein probe into the solution containing 9 times as much non-radioiodine-labeled protein. The de-

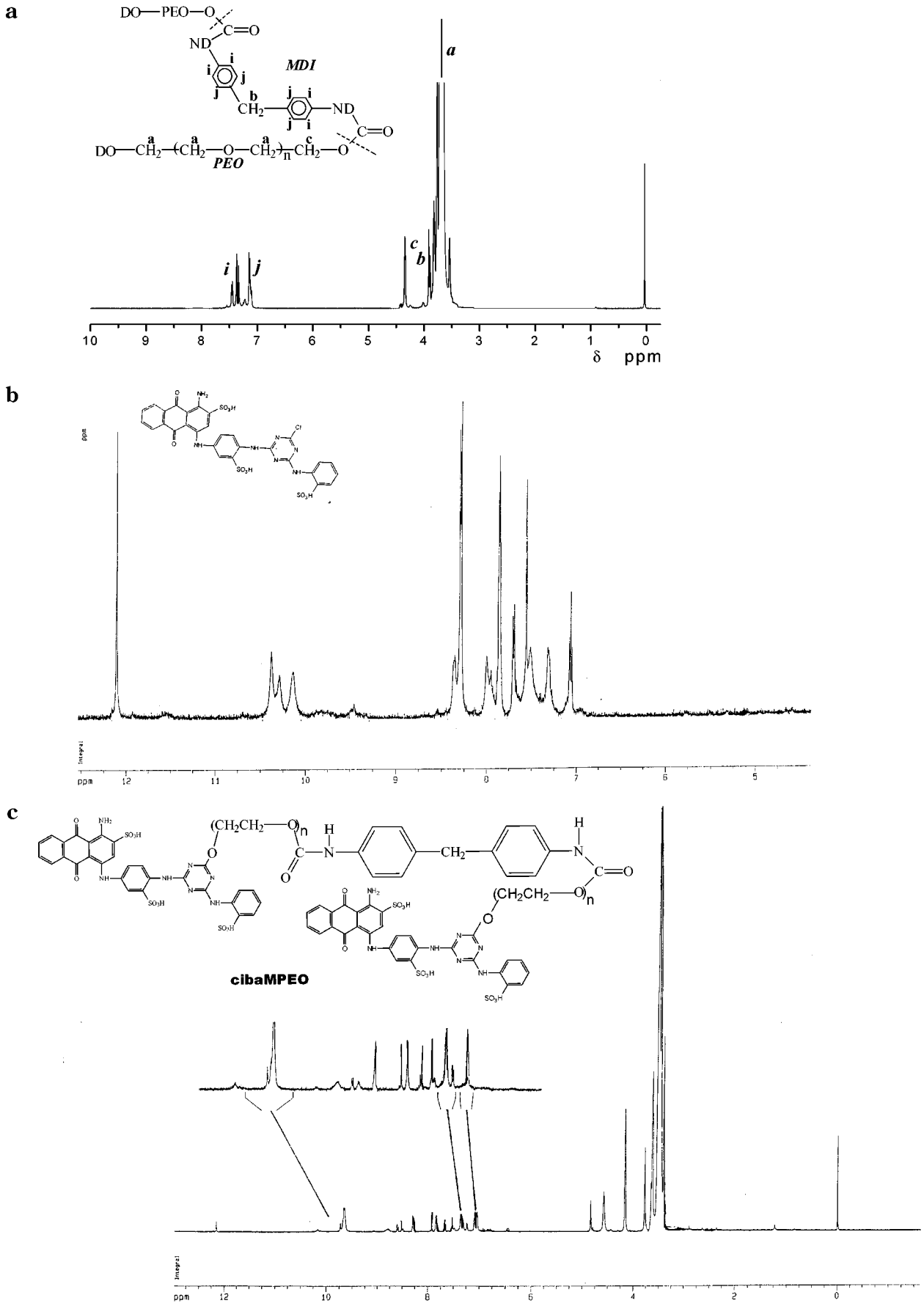

Figure 2. ^{1}H NMR spectra: (a) MPEO(2k), (b) Cibacron Blue F3G-A and (c) cibaMPEO(2k).

termination of concentration was performed through an ultraviolet (Beckman DU-50) method (*18*).

Adsorption Experiment. The modified sheets were previously equilibrated in water for 2 h, and the method

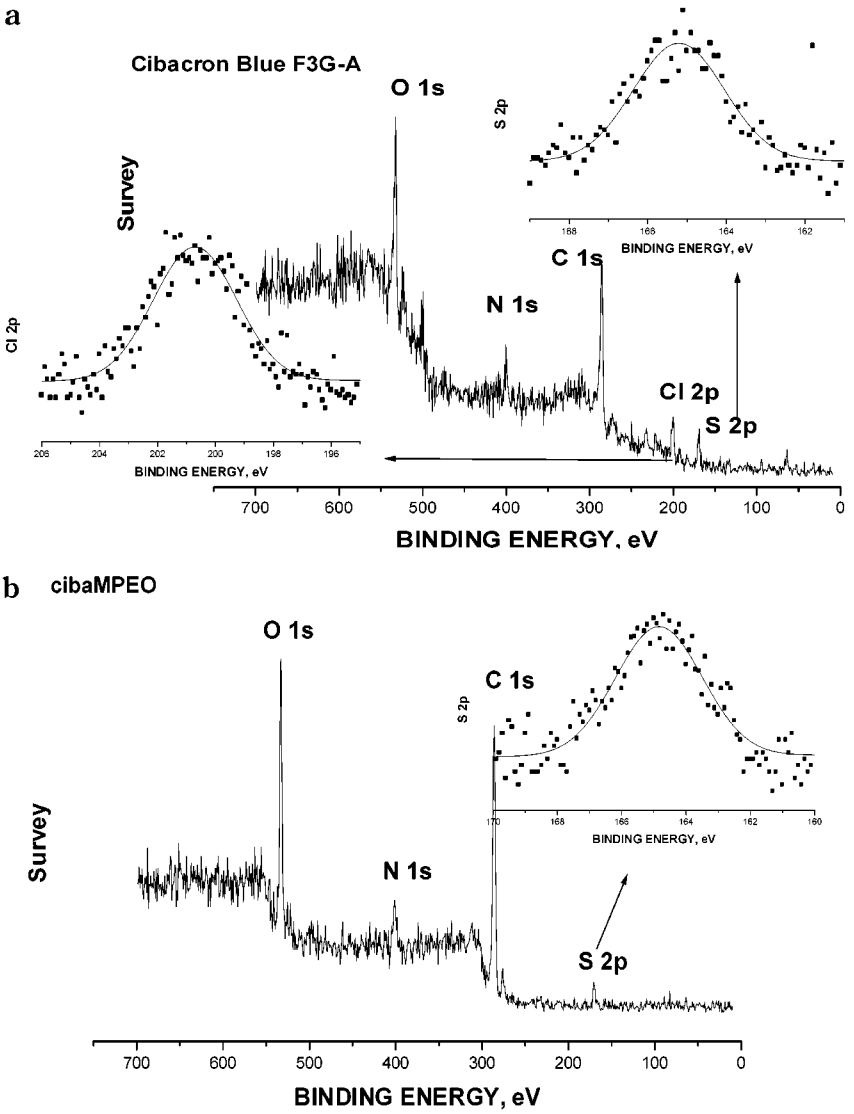

Figure 3. Survey XPS spectra of the powders: (a) Cibacron Blue F3G-A and (b) cibaMPEO(2k).

of adsorption followed a static immersing process in the protein-bulk-solution at 37 °C. After immersion, the residual solution on the surface of the samples was thoroughly removed by a centrifugal method instead of the popular rinsing method with protein-free buffer, to avoid the undesirable protein desorption by leaching and to maintain the original status on the polymer surfaces in the protein solution.

ATR-FTIR Analysis of BSA-Adsorbed Surfaces. ATR-FTIR (E.S.P., MAGNA-IR560, Nicolet; two types of ATR fittings respectively for solid samples (Scheme 3a) and solution (Scheme 3b); IRE crystal: ZnSe, sampling interface 80 mm × 10 mm, refractive index $n_1 = 2.42$, infrared internal reflecting angle *(θ)* 45°) was used to quantitatively characterize the adsorbed proteins (non-radioiodine-labeled). Thirty-two scans were performed. The blank sheet without BSA (or the solvent) was prescanned in a referenced infrared path to yield the background data, the corresponding BSA-adsorbed sample (or the protein solution) was scanned, and the nonprotein background was subtracted off automatically. The correct subtraction should make the region 1900−1720 cm^{-1} flat (*12*). BSA solutions (10.4 mg/mL and 30.6 mg/mL) were used as the parallel standard solution.

Static Isothermal Adsorption. The 5.0 mg/mL, 10.4 mg/mL, and 30.6 mg/mL BSA solutions were employed, and the time of adsorption was 30 min.

Static Adsorption Kinetics. The 30.6 mg/mL BSA solution was employed, and data at six time-points (0.5, 1, 5, 10, 30, and 60 min) were collected.

Adsorption Analysis of ^{125}I-Labeled Proteins A scintillation γ-ray counter (SN 682, Shanghai Institute of Atomic Nucleus) was used to quantitatively characterize the adsorbed proteins (radioiodine-labeled), and the data at six time-points (5, 10, 15, 30, 60, and 90 min) were respectively collected. The standard curve was obtained according to the radiocount from the standard ^{125}I-labeled protein solution.

Adsorption of ^{125}I-Labeled Proteins. The 0.4 mg/mL BSA solution and the 0.04 mg/mL Fg solution were respectively employed.

Selective Binding of Albumin in BSA−Fg Binary Protein System. Parallel adsorption on the same samples was carried out at the same time respectively in radioiodine-labeled BSA/nonlabeled Fg and nonlabeled BSA/radioiodine-labeled Fg binary solutions with the same protein concentrations. The compound results indicated the information of competitive adsorption. Two systems

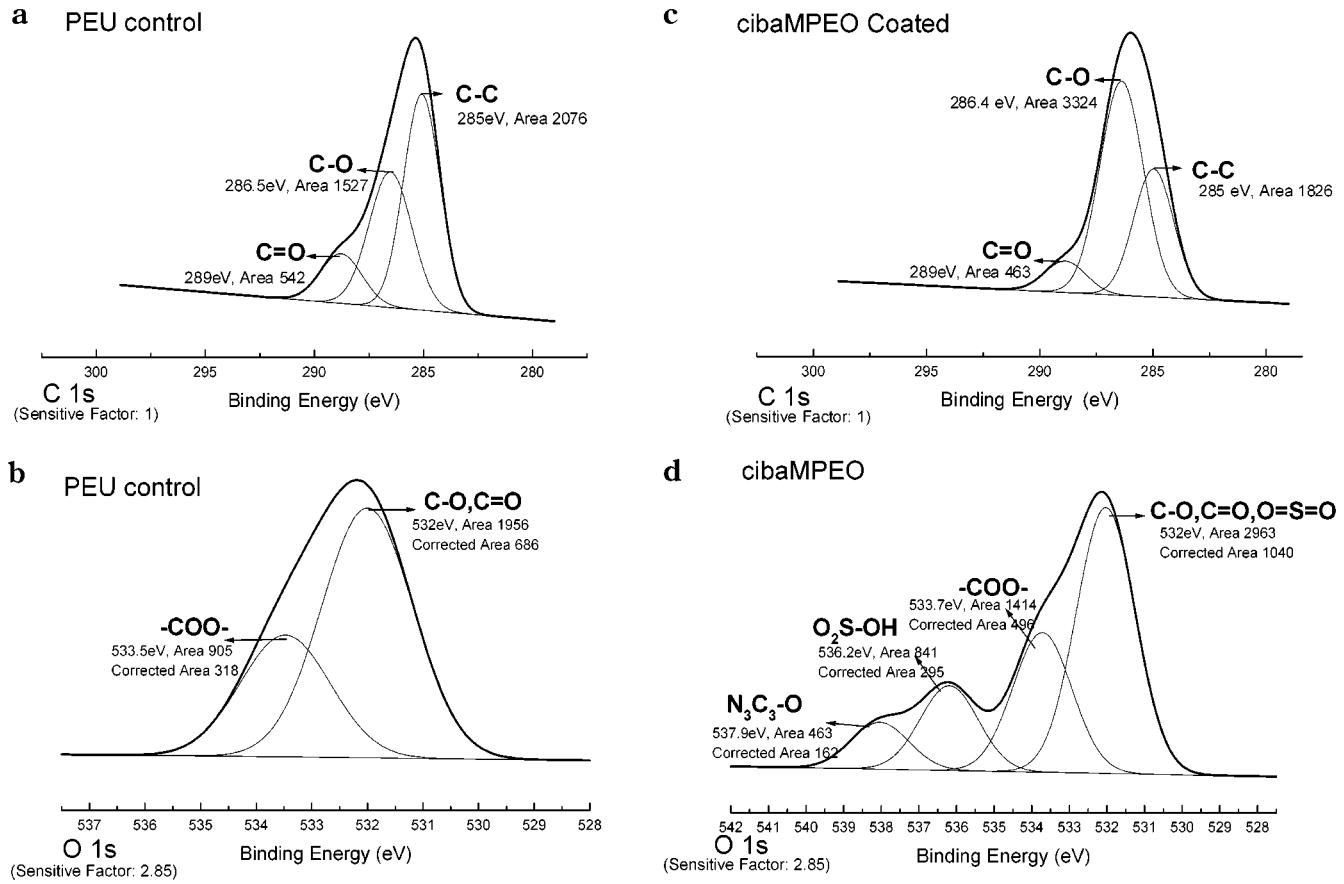

Figure 4. Curve-fit data of the XPS spectra: (a) and (b) respectively C 1s and O 1s peaks of PEU-control; (c) and (d) respectively C 1s and O 1s peaks of ct-cibaMPEO(2k).

of BSA−Fg binary solutions with the concentration of 0.8−0.02 and 0.8−0.06 (mg/mL) were employed, respectively.

Reversibility of Albumin Binding. After the samples had been immersed in 0.4 mg/mL radioiodine-labeled BSA solution for 60 min, the radioactive solution was replaced by non-radioiodine-labeled BSA solution with the same concentration. Then the data at three time-points, 5, 30, and 60 min (65, 90, and 120 min) were collected, respectively.

Plasma Recalcification Time Tests. Human plasma (0.1 mL, blood type B, Central Blood Bank of Hangzhou; containing ACD anticoagulant, without Ca^{2+}) and $CaCl_2$ solution (0.1 mL 0.025 mol/L) were respectively warmed to 37 °C and then were mixed in a test tube whose inner wall had been coated with the SMAs. At the same time, we began to stir the recalcified plasma with a small stainless steel hook and started to time it until the silky fibrin appeared. The duration was recorded as the plasma recalcification time (PRT).

RESULTS AND DISCUSSION

SMA−CibaMPEO and CibaMPEO-Modified PEU Surfaces. *Synthesis and Purification of SMA−CibaMPEO.* As described by Burton et al.,[15] following synthesis, the product was purified several times with ion exchanger. Finally, the dark blue polymeric powder of cibaMPEO was obtained. The GPC data (Figure 1, cibaMPEO2k) indicates that the ciba endgroups have changed the hydromechanical size of whole molecule dramatically, although the M_n of ciba is relatively small. The gradual flatting of the unreacted MPEOs' GPC peak at RT 18.4 min indicates that the product was purified. Figures 2a, 2b, and 2c are the ^{1}H NMR spectra of MPEO2k, ciba, and cibaMPEO2k, respectively, from which it can be observed that the spectrum of cibaMPEO combines all the typical peaks of ciba and MPEO. Moreover, when the XPS spectrain Figures 3a and 3b are compared, ciba powder and cibaMPEO2k powder, respectively, in the cibaMPEO2k spectrum (Figure 3b) the Cl-2p peak at approximately 201 eV has been eliminated, while the S-2p peak at approximately 165 eV is still present. All the data above indicate that the Cl^- of ciba has been nucleophilically substituted by the hydroxyl endgroup of MPEO and that the synthesis shown in Scheme 1 has been accomplished.

Surface Analysis on Modified PEU by XPS. From Figures 4a and 4c, the XPS C-1s region of PEU-control and ct-cibaMPEO2k, respectively, the ratio of C−O (286.5 eV)/C−C (285 eV) increases from 0.736 to 1.820. This ratio on PEU (on the soft blocks, poly(tetramethylene glycol)) is 2/3, while on cibaMPEO (on PEO segments) it is approximately 2; thus, the increase indicates the enrichment of PEO chains on the ct-cibaMPEOs. From Figures 4b and 4d, the XPS O-1s region of PEU-control and ct-cibaMPEO2k, respectively, it is indicated that the components of ciba have been introduced. Furthermore, the radiocount of O/C (has been corrected with the sensitive factor of oxygen 2.85) also has increased from 0.2422 to 0.3551. All of the data confirm the surface-content of both PEO and ciba.

ATR-FTIR Analysis of BSA-Adsorbed Surfaces. Due to the sensitivity and the operating conditions, the quantitative method of ATR-FTIR was specially used to deal with the BSA adsorption in the solution with a high BSA-bulk-concentration. In this paper, the concentration

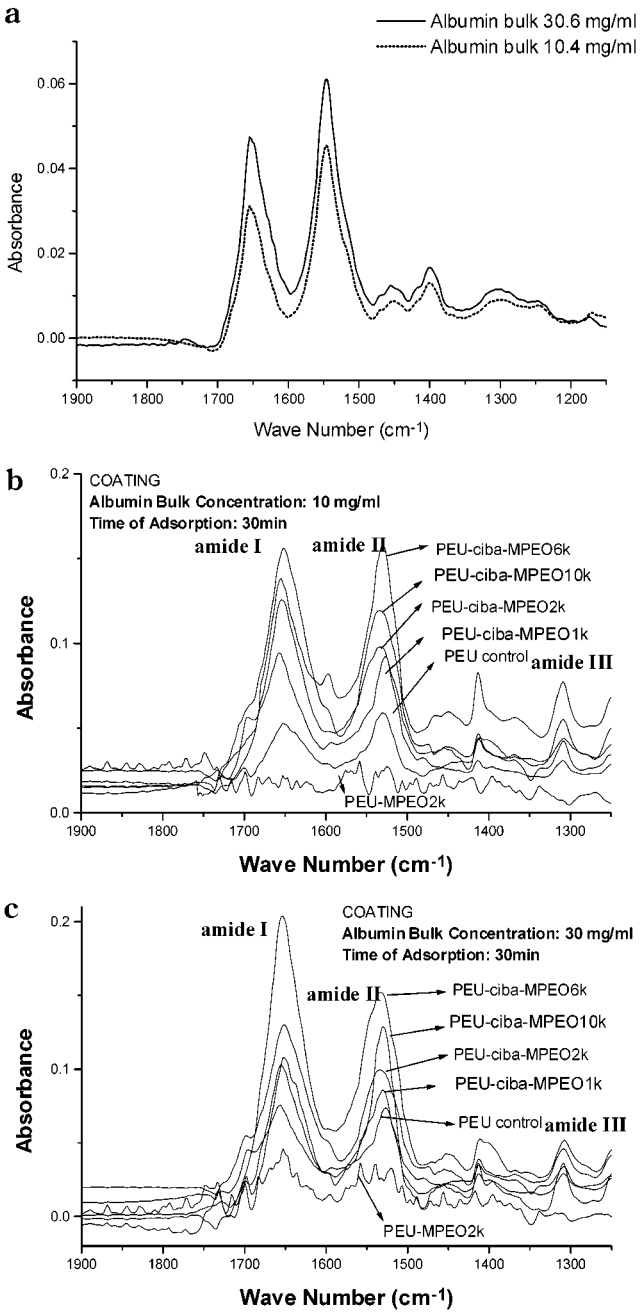

Figure 5. ATR−FT-IR spectra: (a) 30.6 mg/mL and 10.4 mg/ml standard BSA solution; ct-cibaMPEO(2k) from (b) 10.4 mg/mL BSA-bulk-solution and (c) 30.6 mg/ml BSA-bulk-solution.

was as high as 5.0−30.6 mg/mL. On the IR spectra, the integrated area of the protein-typical amide II band at 1550 cm^{-1} was obtained because its peak area can be related to the total amount of protein adsorbed at the interface (*19*, *20*). The horizontal baseline for integration was 1720−1480 cm^{-1}, and the region for integration was 1600−1480 cm^{-1} (*12*). The integrated area A_2 for BSA-adsorbed samples and A_s for standard solution is the average value of six parallel data.

The calculation of the adsorbing density on the modified PEU surfaces is based on the Tompkin equation (*21*),

$$\frac{A}{N}\frac{n_{21}E_0^2\epsilon}{\cos\theta}\int_0^\infty C(z)\exp\left(\frac{-2z}{d_p}\right)dz$$

where A is the integrated absorbance, N is the number of internal reflections, n_{21} is the index of refraction

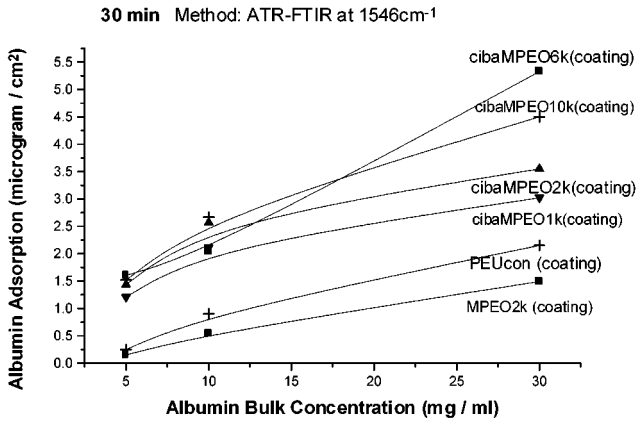

Figure 6. Curves of static isothermal BSA-adsorption: PEU-control, ctMPEO2k, and ct-cibaMPEOs, characterized by ATR-FTIR.

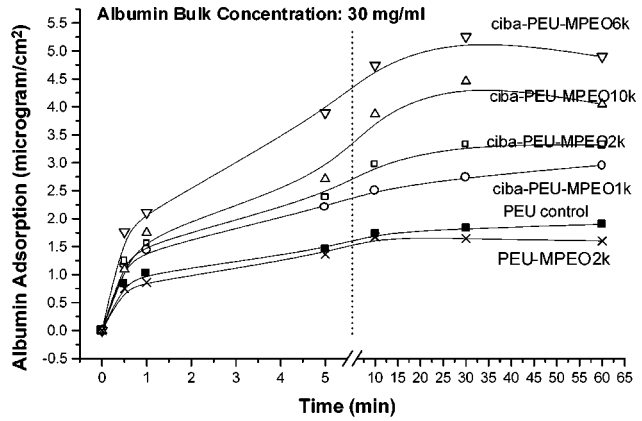

Figure 7. Curves of static BSA-adsorbing kinetics: PEU-control, ctMPEO2k, and ct-cibaMPEOs, characterized by ATR-FTIR.

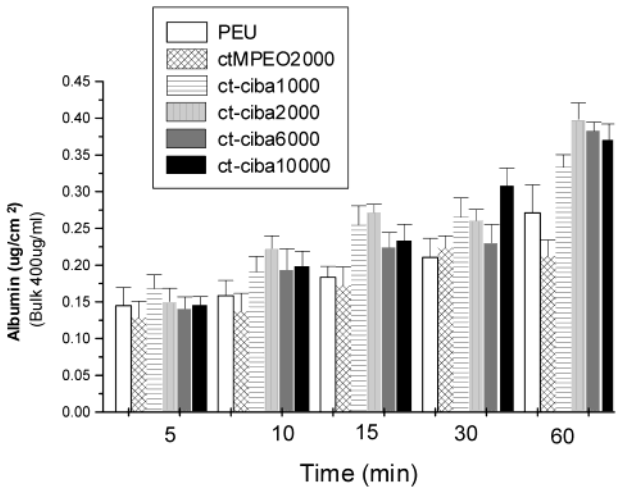

Figure 8. Static BSA-adsorbing data of PEU-control, ctMPEO2k, and ct-cibaMPEOs, characterized by radioactive ^{125}I-probe.

n_2/n_1, ϵ is the integrated molar absorptivity, θ is the incidence angle, $C(z)$ is the concentration as a function of distance z from the interface, E_0 is the electric field amplitude, d_p is the depth of penetration, $d_p = \lambda/[2\pi(n_1^2 \sin^2\theta - n_2^2)^{1/2}]$ (*21*), and λ is the infrared wavelength (6.45 μm, 1550 cm^{-1}). According to the results reported (*5*), besides the dimensions of the PEU sheet surface are exactly equal to that of the IRE testing interface, the

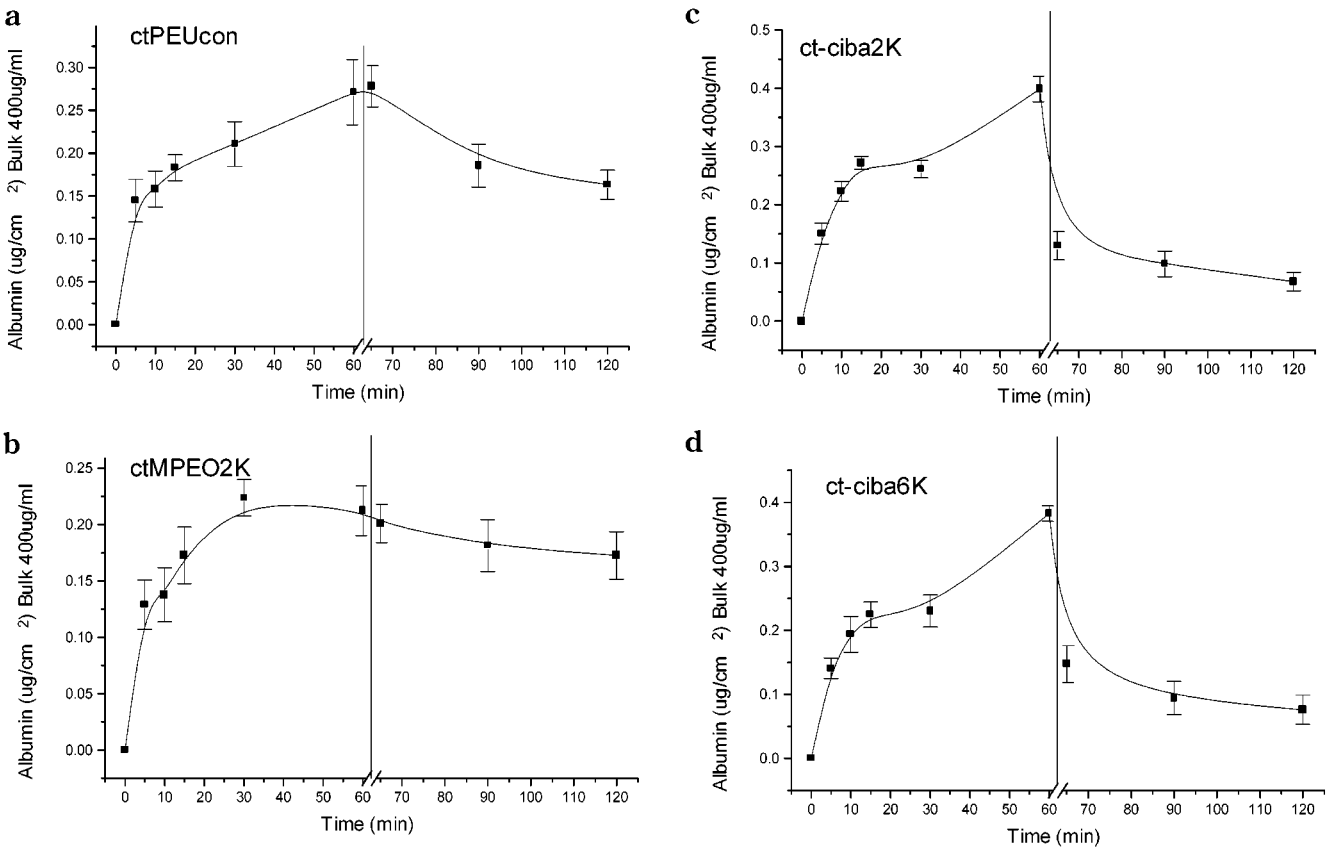

Figure 9. Curves of static BSA-adsorbing kinetics: (a) PEU-control, (b) ctMPEO2k, (c) ct-cibaMPEO2k, and (d) ct-cibaMPEO6k, characterized by radioactive ^{125}I-probe.

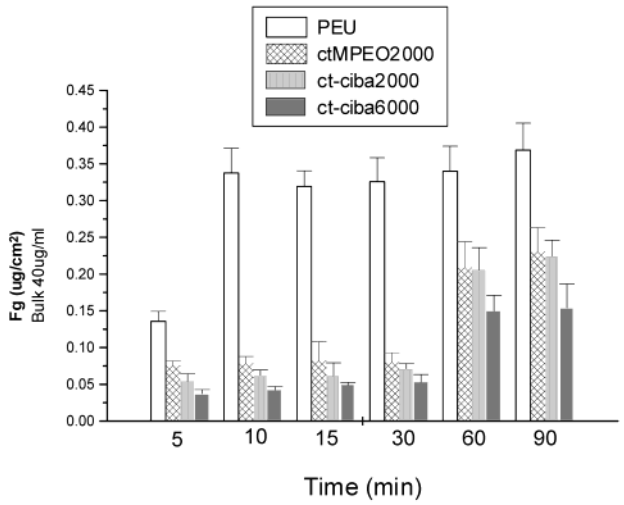

Figure 10. Static Fg-adsorption data of PEU-control, ctMPEO2k, and ct-cibaMPEOs, characterized by radioactive ^{125}I-probe.

equation can be simplified as $\Gamma = A_2C_sd_p/(2A_s)$, where Γ is the density of protein adsorption (μg/cm^2) and C_s is the concentration of standard protein solution.

Figure 5 shows the examples of ATR-FTIR spectra. Figures 5a, 5b, and 5c are respectively the spectra of BSA standard solutions, adsorbed BSA on the sample surfaces in 10.4 mg/mL bulk solution and that in 30.6 mg/mL bulk solution. Figure 6 is the isothermal curves of BSA-adsorption. It is observed that for all the samples, the relation between the amount of adsorbed BSA and the concentration of BSA-bulk-solution (5.0−30.6 mg/mL) is generally a linearly incremental change. In addition, the amount of adsorbed BSA on PEU-control was lower than that on the ct-cibaMPEOs, but higher than that on ctMPEO2k, which indicates the repulsion of the bare PEO chains to the BSA-adsorption and simultaneously demonstrated the outstanding BSA-binding capacity of ciba. The ascending BSA-adsorption from that on ct-cibaMPEO1k to that on ct-cibaMPEO6k indicates that the longer PEO chain is able to provide better support and higher mobility to ciba endgroups, which is due to the intrinsic property of PEO in aqueous environments (*9*). For ciba endgroups, better support from PEO will lead to a higher surface enrichment, and higher mobility means higher activity for BSA-binding. This cooperative effect between PEO spacer and ciba endgroup was approximately best achieved under a PEO-chain-length of 6000. Longer PEO chains such as in PEO10000 cannot significantly produce any more positive effects; on the contrary, the amount of ciba endgroups will inevitably decrease, which is the reason for less BSA-adsorption on ct-cibaMPEO10k than that on ct-cibaMPEO6k. Figure 7 shows the curves for static adsorption kinetics. In the case of 30.6 mg/mL BSA-bulk-concentration, the fast BSA-adsorption happens in the first minute, and then the adsorption slows down; for different samples, a larger amount of adsorbed BSA is obtained, the later the adsorbing saturation is reached.

Adsorption Analysis of ^{125}I-Labeled Proteins. *Adsorption and Reversible Binding of ^{125}I-Labeled BSA.* The amount of adsorbed BSA on each sample is shown in Figure 8. According to the comparison with the case of PEU-control, the PEO chains' repulsive performance and the ciba's BSA-binding capacity, as well as the PEO−ciba cooperative effect, are respectively confirmed by the BSA-adsorbing performances on the ctMPEO and ct-cibaMPEOs. The curves of adsorption under low BSA-

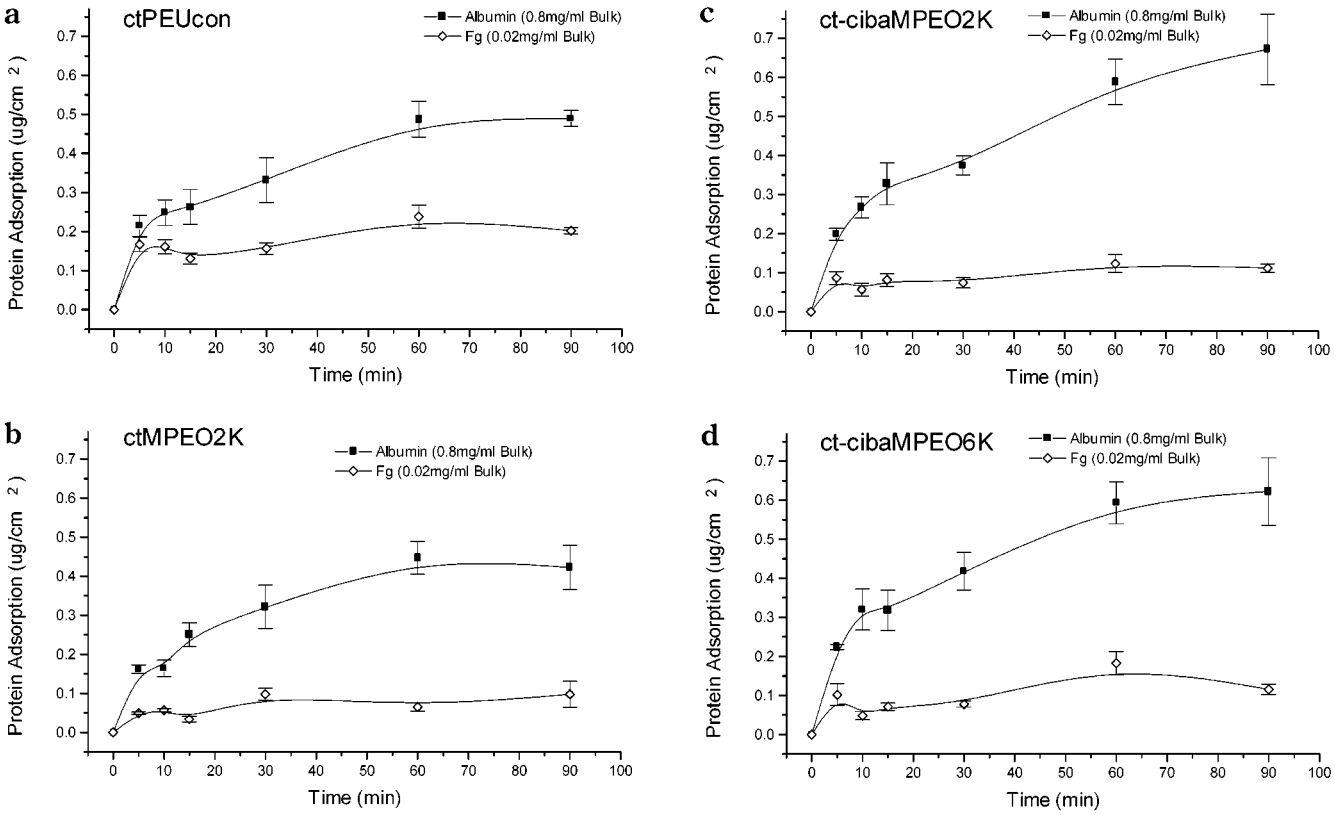

Figure 11. Static BSA−Fg (BSA: 0.8 mg/mL, Fg: 0.02 mg/mL) binary competitive adsorbing kinetics: (a) PEU-control, (b) ctMPEO2k, (c) ct-cibaMPEO2k, and (d) ct-cibaMPEO6k, characterized by radioactive ^{125}I-probe.

bulk-concentration (0.4 mg/ml, shown in Figure 9) demonstrate a similar kinetic adsorbing behavior to that in the high concentration solutions characterized by ATR-FTIR, whereas the difference of BSA-binding capacity between the various samples exhibited under low bulk concentration is not so dramatic as that under high bulk concentration.

The desired effective protein-adsorption is a dynamic equilibrium of adsorption and desorption. Thus, adsorbed proteins with activity can be displaced by the proteins in the bulk solution by probability. Proteins that remain adherent to the polymeric surface permanently are considered irreversibly bound (*22*). Figures 9a and 9b indicate that approximately 41% and 19% of previously bound BSA (radioiodine-labeled) respectively on PEU-control and ctMPEO2k could be displaced in 60 min. From Figures 9c and 9d, it is indicated that approximately 83% and 80% of previously bound BSA (radioiodine-labeled) respectively on ct-cibaMPEO2k and ct-cibaMPEO6k could be displaced within 60 min. Therefore, BSA was reversibly bound to ct-cibaMPEOs, and for ctMPEO2k, despite the high repulsion of PEO, the bound BSA was mostly unrenewable.

Adsorption of ^{125}I-Labeled Fg. Fg was used as a competitive protein because it is known to readily adsorb to implant surfaces and because surfaces that avidly adsorb fibrinogen may be highly thrombogenic (*22*). The amount of adsorbed Fg (bulk-concentration 0.04 mg/mL) on each sample is shown in Figure 10. Within 90 min, the ctMPEO2k and ct-cibaMPEOs bound approximately from 30% to 70% as much ^{125}I-labeled Fg as did PEU-control. The weakest Fg adsorption took place on ct-cibaMPEO6k, and the amounts of the adsorbed Fg on ctMPEO2k and ct-cibaMPEO2k were quite close to each other. All the results listed above indicate that ciba has little special capacity for Fg-binding, while the PEO chains' repulsion to Fg-adsorption has been largely exhibited, and as the dominant factor, the longer the PEO chain length, the higher the repulsion.

Selectivity and Homogeneity of Surface BSA Binding. The direct determination of the extent of preferential binding of BSA to the modified surfaces in the presence of Fg-competition was also performed. The results from the binary BSA−Fg solution with the concentration of 0.8−0.02 (mg mL^{-1}, 40:1 w/w, Bi−Sys I) are shown in Figures 11 and 12, and the results from the 0.8−0.06 system (mg mL^{-1}/mg mL^{-1}, 40:3 w/w, Bi−Sys II) are shown in Figures 13 and 14. The bulk-concentration ratio of BSA to Fg in Bi−Sys II agrees with that ratio in plasma (*23*). From Figures 12b and 14b, it is observed that in the presence of competing Fg, the BSA-adsorbing kinetics on all the surfaces, including PEU-control, ctMPEO2k, and ct-cibaMPEOs, was similar to that in the BSA−one-protein system. As for Bi−Sys I, the curves of competitive adsorbing kinetics (shown in Figure 11) and the ratios of adsorbed-BSA amount to adsorbed-Fg amount (shown in Figure 12a) already can exhibit preferential binding of BSA to the ct-cibaMPEOs. Yet as for Bi−Sys II, the case of more Fg binding than SMA binding on PEU-control was even completely reversed on the ct-cibaMPEOs (shown in Figures 13 and 14a), which can indicate a further dramatic predominance of the homogeneous albumin binding brought by SMA-cibaMPEO.

Plasma Recalcification Time Tests. The results of the PRT tests are shown in Figure 15. Compared with the case of glass and PEU-control, the anticoagulative performance of the modified surfaces was improved, in which the best performance was exhibited on the surfaces modified by cibaMPEO2k-6k. The antithrombogenicity

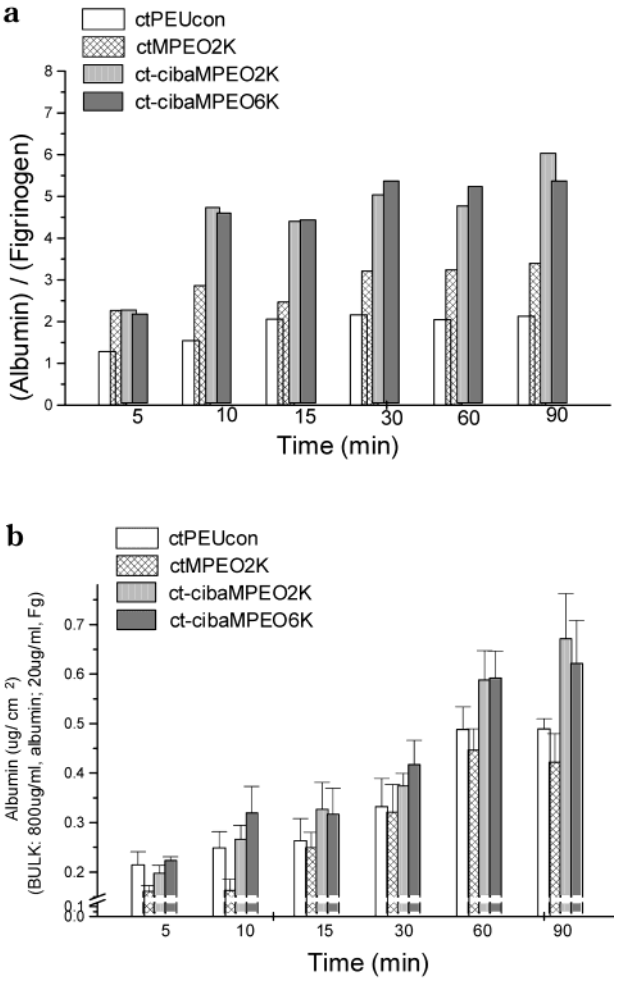

Figure 12. Static BSA−Fg (BSA: 0.8 mg/mL, Fg: 0.02 mg/mL) binary competitive adsorption data of PEU-control, ctMPEO2k, ct-cibaMPEO2k and -6k: (a) ratio of adsorbed BSA amount to adsorbed Fg amount, (b) amount of adsorbed BSA, characterized by radioactive ^{125}I-probe.

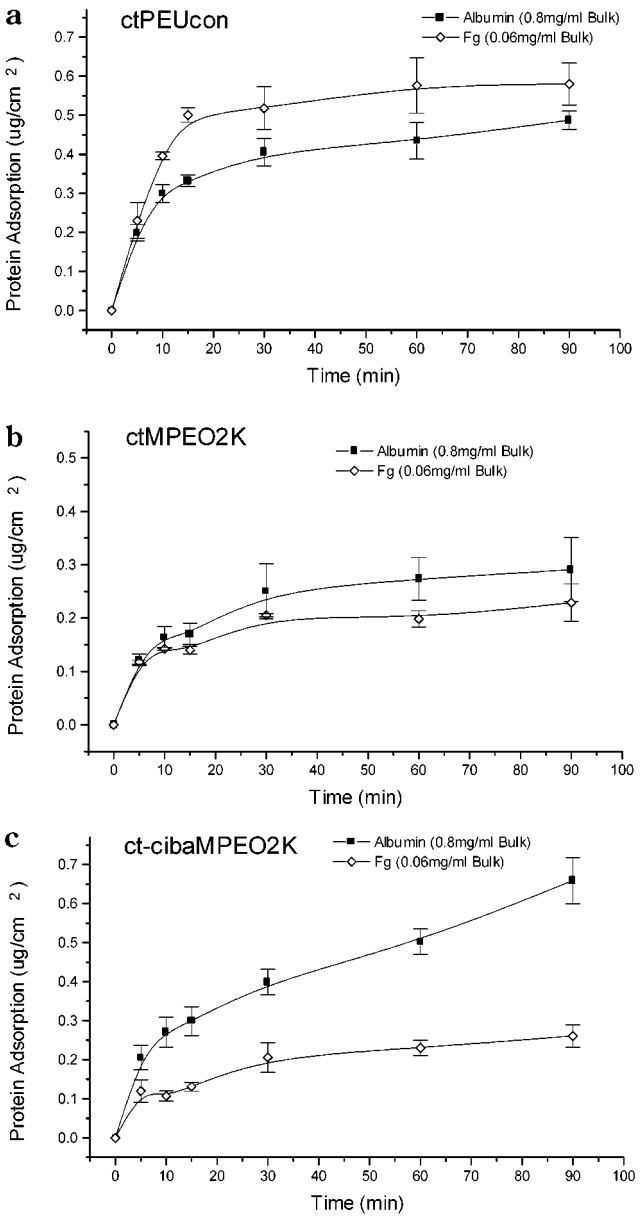

Figure 13. Static BSA−Fg (BSA: 0.8 mg/mL, Fg: 0.06 mg/mL) binary competitive adsorbing kinetics: (a) PEU-control, (b) ctMPEO(2k), and (c) ct-cibaMPEO(2k), characterized by radioactive ^{125}I-probe.

of ct-cibaMPEO1k was similar to that of ctMPEO2k. Along with enlargement of the PEO-chain size from 6k to 10k, the capacity of anti-coagulation decreased. Up to ct-cibaMPEO10k, the anti-coagulative performance was also down to the level of ctMPEO2k. The PRT of the samples is related to the corresponding demonstration of protein adsorption under the competition of albumin−fibrinogen binding. The antithrombogenicity of the cibaMPEOs is originated from the cooperation between ciba endgroups and the PEO spacer, which is due to the coeffect of the exclusion of the thrombogenic proteins and cells plus the selective binding of the inert and biocompatible albumin. While for MPEO2k, it is only from the nonspecifically repulsive function of PEO. On one hand, too long a PEO spacer would make the surface ciba-content limited and the albumin binding would be limited, but on the other hand too short a PEO spacer would immobilize the ciba endgroups and make them less active. Therefore, the cooperative effect between ciba and PEO would finally act on the antithrombogenicity of the modified surfaces.

CONCLUSIONS

In this study, the SMA−cibaMPEOs were synthesized, and the cibaMPEO-modified PEU surfaces were prepared by dip-coating. The surface analysis by XPS revealed the surface enrichment of both ciba and PEO. On the modified surfaces, the quantitative analysis of serum proteins' adsorption was performed. The BSA-adsorption respectively in the low and high BSA bulk-concentration solutions was correspondingly characterized by the methods of radioactive ^{125}I-probe and ATR-FTIR. The Fg-adsorption in the Fg bulk solution and the BSA−Fg competitive adsorption in the BSA−Fg binary solutions were also characterized utilizing the radioactive ^{125}I-probe. Finally the blood compatibility of the modified surfaces was examined by PRT tests.

According to the results of the two independent methods, the BSA-adsorbing kinetics curves of the samples both in the low and high BSA-bulk-concentration solutions, as well as including that in the BSA−Fg binary solutions, were respectively exhibited to be similar to each other. The only difference observed was the higher BSA adsorption in the high BSA-bulk-concentration solution. The comparison between the protein-adsorbing results on PEU-control, ctMPEO2k, and the ct-cibaMPEOs indicates that ciba has a high capacity of selectively

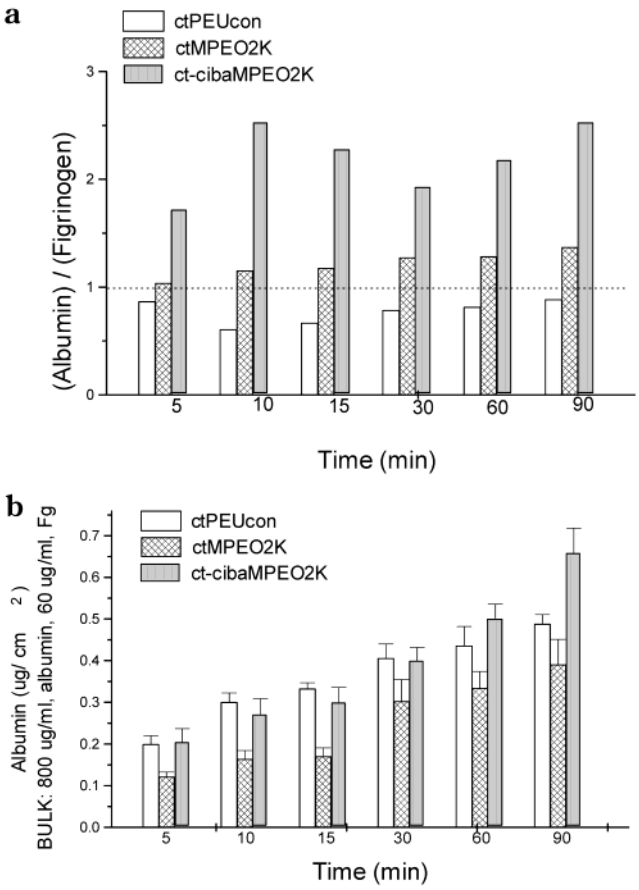

Figure 14. Static BSA-Fg (BSA: 0.8 mg/mL, Fg: 0.02 mg/mL) binary competitive adsorption data of PEU-control, ctMPEO-(2k), and ct-cibaMPEO(2k): (a) ratio of adsorbed BSA amount to adsorbed Fg amount, (b) amount of adsorbed BSA, characterized by radioactive ^{125}I-probe.

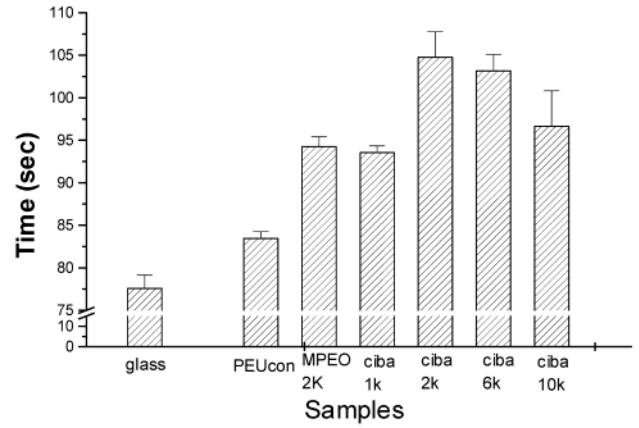

Figure 15. Plasma recalcification time data of glass, PEU-control, ctMPEO(2k), ct-cibaMPEOs.

binding albumin, while PEO can nonspecifically repulse both of the protein adsorption. Whether in a competitive binary protein system or in a one-protein system, the achievement of the albumin-coated surface depends on the demonstration of the cooperative effects between the functional endgroup ciba and the PEO spacer. If the hydrophilic and mobile PEO spacer is too short like PEO1k, it could not sufficiently support and activate the ciba endgroup in the aqueous environment. If the PEO spacer is too long like PEO10k, the surface content of ciba endgroups will inevitably be reduced and the folding of long-chain PEO will also decrease the chain mobility. The results indicate that the remarkable coeffect between the nonspecific repulsion by PEO spacer and the reversibly selective albumin-binding by ciba endgroups is achieved on cibaMPEO2k and -6k, and accordingly, good blood compatibility was also obtained.

ACKNOWLEDGMENT

This research is financially supported by Ministry of Education, National Natural Science Foundation (NSFC 29804009) and National Basic Science Research and Development Grants (No. G1999054305) of the People's Republic of China.

LITERATURE CITED

(1) Lelah, M. D., and Cooper, S. L. (1986) *Polyurethanes in Medicine*, p 57, CRC Press, Boca Raton, FL.
(2) Ikada, Y. (1984) *Advances in Polymer Science*, Vol. 57, p 103, Springer, Berlin.
(3) Han, D. K., Park, K. D., Rug, G. H., Kim, U. Y., Min, B. G., and Kim, Y. H. (1996) Plasma protein adsorption to sulfonated poly(ethylene oxide) grafted polyurethane. *J. Biomed. Mater. Res. 30*, 23−30.
(4) Aldenhoff, Y. B. (1995) Studies on a new strategy for surface modification of polymeric biomaterials. *J. Biomed. Mater. Res. 29*, 917−928.
(5) Pitt, W. G., and Cooper, S. L. (1988) Albumin adsorption on alkyl chain derivatized polyurethanes: I. The effect of C-18 alkylation. *J. Biomed. Mater. Res. 22*, 359−382.
(6) Pitt, W. G., Grasel, T. G., Cooper, and S. L. (1988) Albumin adsorption on alkyl chain derivatized polyurethanes, II. The effect of alkyl chain length. *Biomaterials 9*, 36−43.
(7) He, M. X., and Carter, D. C. (1992) Atomic structure and chemistry of human serum albumin. *Nature 358*, 209−214.
(8) Keogh, J. R., and Eaton, J. W. (1994) Albumin binding surfaces for biomaterials. *J. Lab. Clin. Med. 124*, 537−545.
(9) Llanos, G. R., and Sefton, M. V. (1993) Does poly(ethylene oxide) possess a low thrombogenicity. *J. Biomater. Sci. Polym. Edn. 4*, 381−400.
(10) Wang, D. A., Ji, J., and Feng, L. X. (2000) Surface analysis of poly (ether urethane) blending stearyl poly (ethylene oxide) coupling-polymer. *Macromolecules 33*, 8472−8478.
(11) Wang, D. A., Ji, J., and Feng, L. X. (2000) Various-sized stearyl poly (ethylene oxide) coupling-polymer blending Poly (ether urethane) material for surface study and biomedical applications. *Macromol. Chem. Phys. 201*, 1574−1584.
(12) Chittur, K. K. FTIR/ATR for protein adsorption to biomaterial surface. (1998) *Biomaterials 19*, 357−369.
(13) Fink, D. J., Hutson, T. B., Chittur, K. K., and Gendreau, R. M. Quantitative surface studies of protein adsorption by infrared spectroscopy II. quantification of adsorbbed and buik proteins. *Anal. Biochem.* **1987**, *165*, 147−154.
(14) Wang, Z. Y., Li, J. Z., and Ruan, C. G. (1996) *Thrombogenic and Haemostatic Fundamental Theoretics and Clinical Practice*, 2nd ed., p 280, Shanghai Sci., & Technol Press, Shanghai.
(15) Burton, S. J., McLoughlin, S. B., Stead, C. V., and Lowe, C. R. (1988)Design and applications of biomimetic anthraquinone dyes I. Synthesis and characterization of terminal ring isomers of C. I. reactive blue 2. *J. Chromatogr. 435*, 127−137.
(16) Ratner, B. D., Yoon, S. C., Kaul, A., and Rahman, R. (1987) *Polyurethanes in Biomedical Engineering II* (H. Planck, I. Syre, M. Dauner, and G. Egbers, Eds.) p 231, Elsevier, Amsterdam.
(17) Brash, J. L., and Davidoson, V. J. (1976) Adsorption of glass and polyethylene from solutions of fibrinogen and albumin. *Thromb. Res. 9*, 249−259.
(18) Lin, J. C. (1988) *Haemo-Biochemistry*, p 409, People's Health Press, Beijing.
(19) Miyazawa, T. (1980) *Infrared Spectra and Helical Conformation in Poly-α-Amino Acids* (G. D. Fasman, Ed.) p 1, Marcel Dekker, New York.
(20) Jeon, J. S., Sperline, R. P., and Raghavan, (1992) S. Quantitative Analysis of Adsorbed Serum Albumin on Seg-

mented Polyurethane Using FT-IR/ATR Spectroscopy. *Appl. Spectrosc. 46*, 1644−1648.
(21) Harrick, N. J. (1967) *Internal reflection spectroscopy*, Interscience, New York.
(22) Chinn, J. A., Horbett, T. A., and Ratner, B. D. (1992) Baboon fibrinogen adsorption and platelet adhesion to polymeric materials. *Thromb Haemost. 65*, 608−617.
(23) Elbert, D. L., and Hubbell, J. A. (1996) Surface treatments of polymers for biocompatibility. *Annu. Rev. Mater. Sci. 26*, 365−394.

BC0255079